Proceedings of "Applications of Physics in Mechanical and Material Engineering" (APMME 2024)

Simulation and Measurements of Magnetocaloric Effect in the MnCoGe Modified by Zn

K. Kutynia[a,*], A. Przybył[a], I. Bialik[a], A. Kiljan[b] and P. Gębara[a]

[a] *Department of Physics, Faculty of Production Engineering and Materials Technology, Czestochowa University of Technology, al. Armii Krajowej 19, 42-200 Częstochowa, Poland*
[b] *Department of Department of Materials Engineering and Biomaterials, Faculty of Mechanical Engineering, Silesian University of Technology, Konarskiego 18a, 44-100 Gliwice, Poland*

Doi: 10.12693/APhysPolA.147.262 *e-mail: karolina.kutynia@pcz.pl

In the present paper, the theoretical simulation and experimental studies of magnetic properties of the $Mn_{0.9}Zn_{0.1}CoGe$ alloy was done. Field dependences of magnetization in a wide range of temperatures were collected. Based on the thermomagnetic Maxwell relation, the magnetic entropy change ΔS_M was calculated. Moreover, using the phenomenological model, temperature dependences of magnetization in a wide range of fields were simulated. Values of thermomagnetic properties, such as magnetic entropy change and refrigeration capacity, were calculated.

topics: MM'X alloy, magnetocaloric effect (MCE), X-ray diffraction (XRD), magnetocaloric properties

1. Introduction

The magnetocaloric effect (MCE) described as an adiabatic temperature change (ΔT_{ad}) consists of two stages, i.e., heating during magnetization and cooling during demagnetization [1]. The first mentions of the magnetocaloric effect appeared already in 1860, when W. Thomson described the theoretical predictions of the occurrence of this phenomenon [2]. Then, in 1917, P. Weiss and A. Piccard [3] described and discovered MCE. In 1926, P. Debye [4] and 1927 W. Giaque [5] explained the mechanism and practical application of MCE to achieve very low temperatures in the process of adiabatic demagnetization of paramagnets. But it is since 1997, after the discovery of a giant MCE in $Gd_5Ge_2Si_2$ alloys by V. Percharsky and K. Gschnaider Jr. [6], that we observed a huge interest in the subject of cooling using the magnetocaloric effect.

Mn–Co–Ge alloys belong to the MM'X alloy group, where: M and M' — transition metals, X — element from the main group. These alloys are characterized by ferromagnetic martensitic transition (FMMT). They crystallize in two phases, i.e., high-temperature hexagonal Ni_2In type (space group $P6_3/mmc$) and low-temperature rhombic NiTiSi type (space group $Pnma$), which is accompanied by a magnetic transition [7].

The magnetic moments of magnetocaloric materials are strongly related to the crystal structure. They cause magnetic transitions to couple with discontinuous changes in crystal symmetry or lattice parameters. These systems can exhibit a gigantic magnetocaloric effect around first-order magnetostructural phase transitions. The magnetostructural coupling occurring in these materials can lead to the appearance of an enhanced magnetocaloric effect even if no such first-order transition occurs [8].

An interesting model, allowing to determine the magnetocaloric properties, was proposed by Hamad in [9].

In our previous articles, we studied the effect of partial substitution of Mn by Zr [10], Pd [11], Nb [12], W [13] in the MnCoGe base alloy. These studies focused on the effect of Zn addition on the change of structure and thermomagnetic properties.

2. Sample preparation and experimental details

Samples with nominal composition of $Mn_{0.9}Zn_{0.1}CoGe$ were prepared using arc melting method of high-purity elements in an Ar protective gas atmosphere. The samples were remelted several times in order to ensure their homogeneity [14, 15]. X-ray diffraction (XRD) studies were performed

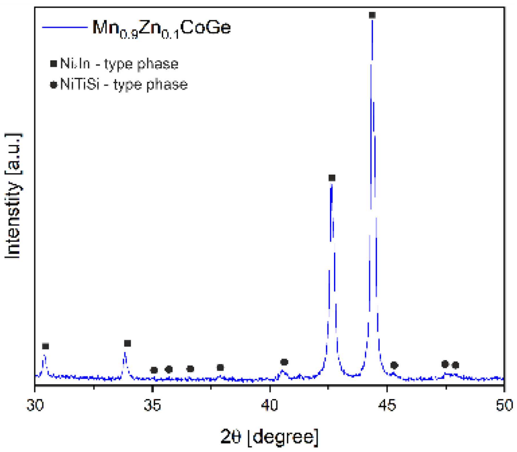

Fig. 1. X-ray diffraction pattern collected at room temperature for the $Mn_{0.9}Zn_{0.1}CoGe$ alloy.

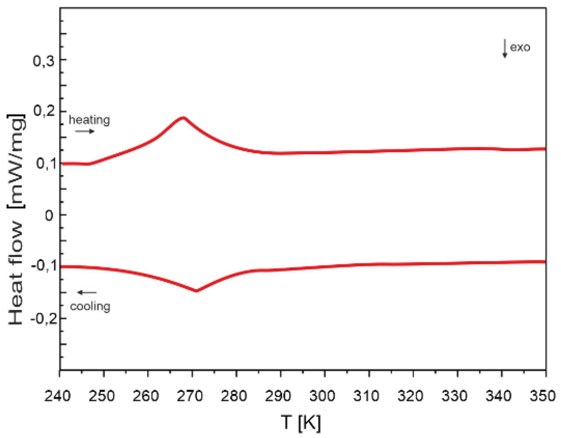

Fig. 2. DSC curve of the $Mn_{0.1}Zn_{0.9}CoGe$ alloy.

using a Bruker D8 Advance diffractometer (Bruker, Karlruhe, Germany) with Cu K_α radiation and a LynxEye semiconductor detector (Bruker, Karlruhe, Germany). The collected X-ray pattern was analyzed with Bruker EVA software (4.3). Rietveld analysis was conducted using the PowderCell 2.4 package [16]. Magnetic measurements were carried out using Quantum Design Physical Properties Measuring System (PPMS) model 6000, equipped to work with a wide range of magnetic fields and temperatures. The full mathematical description of the phenomenological model was given in [9, 17].

3. Results and discussion

A slight increase in lattice constants is evident with the increase in Zn content in the alloy composition. Such an effect is related to the different ionic radius of Zn ($r_{\mathrm{Zn}} = 1.37$ Å) compared to the much smaller radius of Mn ($r_{\mathrm{Mn}} = 1.18$ Å). The in-depth analysis of XRD patterns did not detect

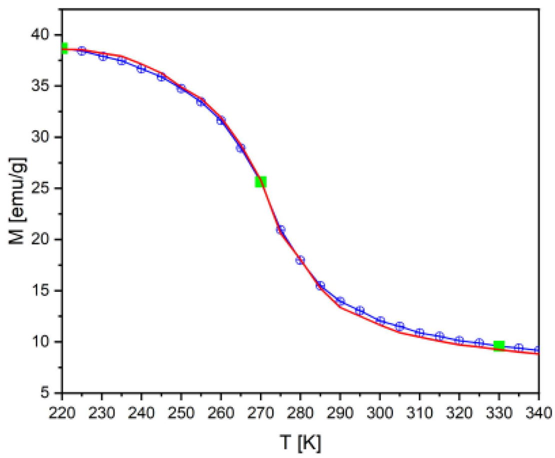

Fig. 3. Temperature dependence of magnetization for the $Mn_{0.9}Zn_{0.1}CoGe$ alloy.

any additional phase associated with the presence of impurities (Fig. 1). Qualitative and quantitative analysis supported by Rietveld analysis performed using experimental XRD patterns revealed a slight change in the lattice constants of the identified phases. The values of the lattice parameters for the high-temperature hexagonal phase of the Ni_2In type are $a = 4.056$, $c = 5.189$, and for the low-temperature rhombic phase of the NiTiSi type the values of the lattice parameters are $a = 5.874$, $b = 3.826$, $c = 7.064$.

In order to confirm the results of XRD analysis and to determine the temperatures of structural and magnetic transitions, differential scanning calorimetry (DSC) measurements were performed (Fig. 2). Exothermic and endothermic peaks were detected in the investigated alloy, as well as a lambda peak corresponding to the Curie temperature.

This temperature is consistent with the Curie temperature expressed by the M vs T curve. In addition, an apparent temperature hysteresis was observed, which was confirmed by thermomagnetic measurements (Fig. 3). The M vs T relationship measured in an external magnetic field up to 0.1 T for the test sample is shown in Fig. 3. The first derivative of the $M(T)$ relation yielded the Curie temperature value. The minimum of the $\mathrm{d}M(T)/\mathrm{d}T$ curve allowed an estimate of the Curie point, which was 275 ± 1 K.

The magnetocaloric effect was investigated indirectly by calculating the change in magnetic entropy ΔS_M. To calculate the value of ΔS_M, magnetic isotherms were measured for a wide range of temperatures. The magnetic entropy change calculations were performed using Maxwell's relation [18]

$$\Delta S_M(T, \Delta H) = \int_0^H \mathrm{d}H \, \left(\frac{\partial M(T,H)}{\partial T}\right)_H, \qquad (1)$$

where H is the magnetic field strength, M is the magnetization, and T is the temperature.

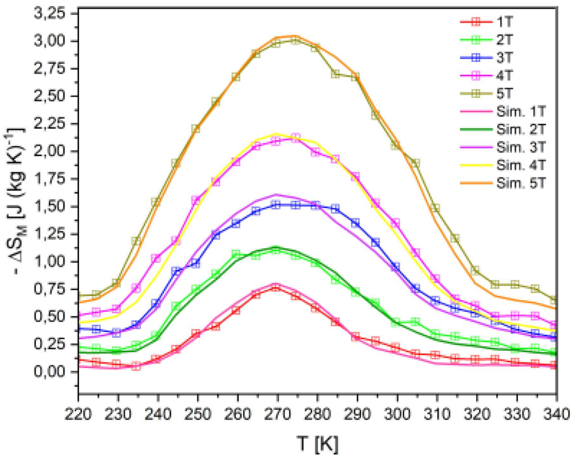

Fig. 4. Temperature dependence of magnetic entropy change for experimental data and simulations over a wide field range.

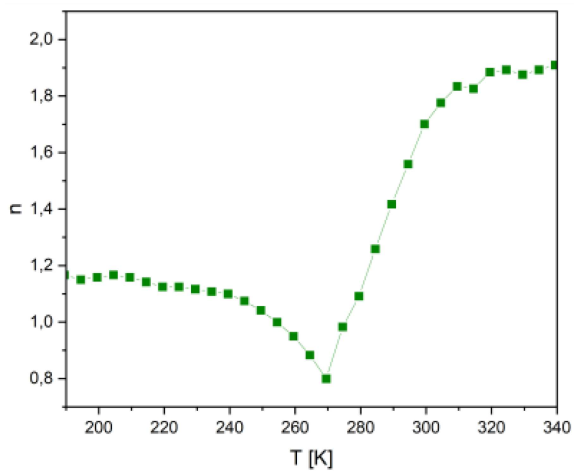

Fig. 5. Temperature evolution of the exponent n revealed for the $Mn_{0.9}Zn_{0.1}CoGe$.

TABLE I

The magnetic field change $\Delta(\mu_0 H)$ and the theoretical and experimental magnetic entropy change ΔS_M (respectively denoted as ΔS_{Mt} and ΔS_{Me}) for the $Mn_{0.9}Zn_{0.1}CoGe$ alloy.

$\Delta(\mu_0 H)$ [T]	ΔS_{Mt} [J/(kg K)]	ΔS_{Me} [J/(kg K)]
1	0.80	0.77
2	1.13	1.11
3	1.61	1.52
4	2.16	2.12
5	3.05	3.01

Equation (1) was implemented in Mathematica software using the following algorithm

$$\Delta S_M\left(\frac{T_i+T_{i+1}}{2}\right) \simeq \frac{1}{T_{i+1}-T_i}\left[\int_0^{B_{\max}} \mathrm{d}B\ M(T_{i+1},B) - \int_0^{B_{\max}} \mathrm{d}B\ M(T_{i+1},B)\right], \quad (2)$$

where B is the magnetic field induction according to the relation $B = \mu_0 H$.

The temperature course of the change in magnetic entropy of the $Mn_{0.9}Zn_{0.1}CoGe$ alloy is shown in Fig. 4. The measurement of ΔS_M values involves measuring magnetic isotherms for a wide range of temperatures. The highest experimental ΔS_M value calculated for an external magnetic field change of ~ 5 T was 3.01 J/(kg K), and the theoretical value of ΔS_M was 3.05 J/(kg K). Compared to the results for the MnCoGe base alloy presented in [19], the addition of Zn caused a slight decrease in ΔS_M. The calculated values for the experimental and theoretical magnetic entropy change are summarized in Table I.

The value of relative cooling power (RCP) was also calculated, using the following formula [20]

$$\mathrm{RCP} = \Delta S_M\, \delta T_{\mathrm{FWHM}}, \quad (3)$$

where RCP is the relative cooling power, ΔS_M is the magnetic entropy change, δT_{FWHM} is the half-width of the peak of the magnetic entropy change. For the simulation carried out at an external magnetic field of 5 T, the value of RCP is equal to 122 J/kg, and the value of RCP calculated for the experiment at an external magnetic field of 5 T was 120.4 J/kg.

In [21], Law and Franco proposed a method based on the phenomenological dependence of the magnetic entropy change (ΔS_M) on the field described by the formula

$$\Delta S_M = C\,(B_{\max})^n, \quad (4)$$

where C is the proportionality constant depending on temperature, and n is an exponent strongly dependent on the magnetic ordering of the specimen. Calculation of the exponent n is possible by modifying (4) in the form that was proposed in [22], i.e.,

$$\ln(\Delta S_M) = \ln(C) + n \ln(B_{\max}). \quad (5)$$

In the paper [23], it was shown that the exponent n is slightly dependent on the magnetic ordering of the material. Assuming that the material under study obeys the Curie–Weiss law, the exponent should be 1 and 2 in the ferromagnetic and paramagnetic states, respectively. The value of the exponent n at the Curie temperature is strongly related to the critical exponents and can be written in the following form

$$n = 1 + \frac{1}{\delta\,(1-1/\beta)}, \quad (6)$$

where β and δ are critical exponents.

The temperature dependence of the exponent n is shown in Fig. 5.

4. Conclusions

The purpose of this paper was to carry out theoretical simulation and experimental studies of magnetic properties of the $Mn_{0.9}Zn_{0.1}CoGe$ alloy. The coexistence of high-temperature hexagonal phases of the Ni_2In type and low-temperature rhombic phases of the NiTiSi type was detected in the studied alloy. Analyzing the results obtained for the experimental data, as well as those obtained during simulation, it can be seen that the simulation values coincide with the experimental data. This means that the parameters selected in the simulation correspond to the actual tests. The effect of Zn addition on the change in T_C value was found to be 275 ± 1 K. The highest experimental ΔS_M value was 3.01 J/(kg K) and the theoretical ΔS_M value was 3.05 J/(kg K) for the $Mn_{0.9}Zn_{0.1}CoGe$ alloy in an external magnetic field of 5 T. For the simulation carried out with an external magnetic field of 5 T, the RCP value is equal to 122 J/kg, and the RCP value calculated for the experiment with an external magnetic field of 5 T was 120.4 J/kg.

References

[1] K.A. Gschneidner, V.K. Pecharsky, *Int. J. Refrig.* **31**, 945 (2008).

[2] W. Thomson, *Cyclopedia of the Physical Sciences*, 2nd ed., Ed. J.P. Nichol, 1860.

[3] P. Weiss, A. Piccard, *J. Phys (Paris)* **5**, 103 (1917).

[4] P. Debye, *Ann. Phys. (Leipzig)* **386**, 1154 (1926).

[5] W.F. Giauque, *J. Am. Chem. Soc.* **49**, 1864 (1927).

[6] V.K. Pecharsky, K.A. Gschneidner Jr., *Phys. Rev. Lett.* **78**, 4494 (1997).

[7] S.C. Ma, Q. Ge, Y.F. Hu et al., *Appl. Phys. Lett.* **111**, 192406 (2017).

[8] T. Hahn, *International Tables for Crystallography, Vol. A: Space Group Symmetry*, Springer-Verlag, New York 2002.

[9] M.A. Hamad, *Phase Trans.* **85**, 106 (2012).

[10] K. Kutynia, P. Gębara, *Materials* **14**, 3129 (2021).

[11] K. Kutynia, A. Przybył, P. Gębara, *Materials* **16**, 5394 (2023).

[12] K. Kutynia, P. Gębara, A. Przybył, *Arch. Metall. Mater.* **67**, 879 (2022).

[13] K. Kutynia, A. Przybył, P. Gębara, *Acta Phys. Pol. A* **146**, 70 (2024).

[14] W. Łoński, M. Spilka, M. Kądziołka-Gaweł, P. Gębara, A. Radoń, T. Warski, S. Łoński, K. Barbusiński, K. Młynarek-Żak, R. Babilas, *J. Alloys Compd.* **934**, 167827 (2023).

[15] A. Kupczyk, J. Świerczek, M. Hasiak, K. Prusik, J. Zbroszczyk, P. Gębara, *J. Alloys Compd.* **735**, 253 (2018).

[16] W. Kraus, G. Nolze, *Powder Differ.* **13**, 256 (1998).

[17] P. Gębara, R. Gozdur, K. Chwastek, *Acta Phys. Pol. A* **146**, 41 (2024).

[18] V.K. Pecharsky, K.A. Gschneider Jr., *J. Appl. Phys.* **86**, 565 (1999).

[19] P. Gębara, Z. Śniadecki, *J. Alloys Compd.* **796**, 153 (2019).

[20] J. Yang, Y.P. Lee, *J. Appl. Phys.* **102**, 033913 (2007).

[21] J.Y. Law, V. Franco, L.M. Moreno-Ramírez, A. Conde, D.Y. Karpenkov, I. Radulov, K.P. Skokov, O. Gutfleisch, *Nat. Commun.* **9**, 2680 (2018).

[22] K.P. Skokov, K.-H. Müller, J.D. Moore, J. Liu, Y.A. Karpenkov, M. Krautz, O. Gutfleisch, *J. Alloys Compd.* **552**, 310 (2013).

[23] K. Morrison, K.G. Sandeman, L.F. Cohen, C.P. Sasso, V. Basso, A. Barcza, M. Katter, J.D. Moore, K.P. Skokov, O. Gutfleisch, *Int. J. Refrig.* **35**, 1528 (2012).